Q. J. R. Meteorol. Soc. (2006), **132**, pp. 1179–1203 doi: 10.1256/qj.05.51

New version of the TOMCAT/SLIMCAT off-line chemical transport model: Intercomparison of stratospheric tracer experiments

By M. P. CHIPPERFIELD*

Institute for Atmospheric Science, School of Earth and Environment, University of Leeds, UK

(Received 23 March 2005; revised 3 November 2005)

SUMMARY

We describe the development of a new three-dimensional off-line chemical transport model (CTM). The CTM has been produced by combining the existing, and closely related, TOMCAT and SLIMCAT models. The new CTM (TOMCAT/SLIMCAT) has a flexible vertical coordinate which can use both σ-p and σ-θ levels. A novel approach is used for the σ-θ coordinate to ensure a smooth transition between levels. The CTM has different options for calculating vertical transport in the stratosphere, depending on the coordinate chosen. The CTM also has different options for other processes such as advection scheme, radiation scheme and meteorological forcing.

We have used different configurations of the new CTM to perform tests on stratospheric tracer transport. Using ECMWF ERA-40 analyses, the σ-p coordinate model gives a stratospheric age of air which is much too low, and a tropical tape-recorder signal which propagates vertically too rapidly. Changing the coordinates to σ-θ levels, and still using the analyses to calculate the vertical motion, removes spurious vertical mixing and improves the modelled age of air significantly, although it still tends to underestimate the observations. If we use a radiation scheme to calculate the stratospheric diabatic transport in the σ-θ model we get a greater age of air, and the best overall agreement with the observations of age of air from *in situ* data and estimates of the tape-recorder signal from Halogen Occultation Experiment CH_4 and H_2O data. Based on the model results, interannual variability can cause age of air changes of up to $\sim$1 year in the mid/high-latitude lower stratosphere. Similar differences can be caused by changing to winds from the UK Met Office. For the year 2001, where two sets of ECMWF analyses are available, the operational analyses produce a greater stratospheric age of air than the ERA-40 re-analyses.

KEYWORDS: Age of air CTM ECMWF ERA-40 Tape recorder

1. INTRODUCTION

Global three-dimensional (3D) models of atmospheric chemistry and transport are now becoming widely used. These models can be separated into those based on general circulation models (GCMs), which calculate their own winds and temperatures, and so-called 'off-line' chemical transport models (CTMs). Off-line CTMs do not calculate their own winds and temperatures. Instead they read in meteorological fields from either analyses or GCM output. The off-line approach has some advantages over GCM-based models. They are computationally cheaper and, when the model is forced by analyses, the model is constrained to the 'real' meteorological situation which aids comparisons to observations. However, chemical GCMs are needed for studies involving chemical–radiative–dynamical feedbacks and for future predictions. Also, while the 'off-line' approach is simple in principle, there are many issues and potential problems which can affect the success of a model simulation.

Initially, stratospheric and tropospheric CTMs were used for short, seasonal integrations (e.g. Rood *et al*. 1989; Kaye *et al.* 1990; Lefèvre *et al*. 1994). More recently, models have been used for longer simulations. However, while the analysed winds tend to give a good representation of the rapid horizontal transport, they are often not well suited for simulations longer than a few months which depend on the quality of the slow, meridional circulation. Weaver *et al.* (1993) discussed the use of a radiation scheme to resolve some of the problems of vertical winds from assimilated data products. They found that for simulations of many months to years, use of a radiation scheme gave a

* Corresponding address: School of Earth and Environment, University of Leeds, Leeds LS2 9JT, UK.
e-mail: martyn@env.leeds.ac.uk

better representation of the meridional circulation, compared to the analysed vertical winds which were continually being shocked by the assimilation procedure.

The TOMCAT and SLIMCAT off-line CTMs have been widely used for atmospheric chemistry studies over the past decade or so. The TOMCAT model was first described and used by Chipperfield *et al.* (1993) for studies of the polar stratosphere. The TOMCAT model used hybrid σ-p levels; although it performed reasonably well, it was not ideal for stratospheric studies and could not make best use of the stratospheric forcing analyses then available, i.e. those of UK Met Office (UKMO, Swinbank and O'Neill 1994). Therefore, the related SLIMCAT 3D CTM was developed, and first described in Chipperfield *et al.* (1996). This differed from TOMCAT in using an isentropic vertical coordinate (and hence having a domain effectively limited to the stratosphere) and in using diagnosed heating rates to derive the vertical transport. These developments allowed the model to use the UKMO analyses for multiannual stratospheric simulations (e.g. Chipperfield 1999). Meanwhile, the TOMCAT CTM was further developed for tropospheric chemistry studies by the inclusion, for example, of convection (Stockwell and Chipperfield 1999), wet and dry deposition (Giannakopoulos *et al.* 1999), lightning (Stockwell *et al.* 1999) and detailed gas-phase chemistry (Law *et al.* 1998). Effectively SLIMCAT became a stratospheric CTM and TOMCAT, usually forced by ECMWF analyses which then extended to only 10 hPa, a tropospheric CTM.

Recent technical and scientific developments have meant that it would be desirable to combine the two related CTMs into a single model with a flexible vertical coordinate and different methods of treating key processes (e.g. vertical transport). First, in 1999 the ECMWF extended the upper boundary of their analyses to 0.1 hPa and recently completed the ERA-40 re-analyses from 1957 to 2002 over this same domain (Uppala *et al.* 2004). Second, many key scientific issues concern processes in the upper troposphere/lower stratosphere (UT/LS). These include stratosphere–troposphere transport, the composition of the lowermost stratosphere, and processes in the tropical UT. Therefore, model boundaries in the UT/LS region are not desirable.

Other global 3D models have been developed with hybrid vertical coordinates which use isentropic (θ) levels in the stratosphere and terrain-following (σ) levels near the surface. Zapotocny *et al.* (1991) described a hybrid σ-θ GCM but their grid has a discontinuity at the boundary between the two types of level. Thuburn (1993) also described a hybrid σ-θ GCM but with a smooth transition between the levels. Recently, Mahowald *et al.* (2002) described a version of the MATCH off-line CTM in which they had implemented a general hybrid σ-θ coordinate.

This paper describes developments to the original TOMCAT (σ-p) and SLIMCAT (σ-θ) off-line CTMs to produce a new model which extends from the surface upwards with different options for the vertical coordinate. Section 2 describes the new version of the TOMCAT/SLIMCAT model in detail. Section 3 describes the set-up of tracer experiments performed to test various configurations of the model. Section 4 discusses the issue of mass conservation in off-line models. Section 5 discusses the results of the tracer experiments with particular focus on the calculated stratospheric age of air and tropical tape-recorder signal. Conclusions are presented in section 6.

2. THE TOMCAT/SLIMCAT 3D MODEL

This section describes the formulation of the TOMCAT/SLIMCAT 3D CTM. The model uses a global Eulerian grid which extends from pole to pole. The maximum vertical domain is determined by the extent of the analyses (or GCM output) used to force the model, although the model can be run over a shallower depth.

(*a*) *Horizontal grid*

The model grid is variable and determined usually by computational considerations. The longitudinal spacing is regular although the latitudinal spacing can be irregular. The forcing meteorological analyses are generally read in as spectral coefficients (e.g. from ECMWF). These are converted to grid-point fields by a spectral transform which can be done onto any prescribed latitudinal grid using pre-tabulated integrals of the associated Legendre functions. This means that the model is not restricted to the usual Gaussian latitudes. When the model is forced using grid-point winds (e.g. UKMO), the winds are first interpolated to a higher-resolution Gaussian grid and converted to spectral coefficients. The spectral transform to the model grid is then done as for spectral wind fields. Segers *et al.* (2002) recently implemented a similar procedure in their TM5 model, except that they perform the spectral transform of the analyses to a high-resolution Gaussian grid and integrate the resulting grid-point mass fluxes onto the model grid.

(*b*) *Vertical coordinate*

Many GCMs are formulated using a hybrid σ-p vertical coordinate. In this scheme, the model levels vary from pure terrain-following σ levels near the surface to pure pressure levels at higher altitudes (typically above ~100 hPa). The pressure, p, of a model half-level (interface) is then given by

$$p_{k+\frac{1}{2}} = Ap_0 + Bp_s. \tag{1}$$

Consequently many datasets of meteorological analyses are also produced on these hybrid σ-p levels. (The appendix lists the symbols used in this paper.)

In TOMCAT/SLIMCAT, the vertical coordinate of the model levels can be defined in two ways: (i) hybrid σ-p levels ('TOMCAT' mode) or (ii) hybrid σ-θ levels ('SLIMCAT' mode). For hybrid σ-p levels, the definition of the levels follows Eq. (1). For the hybrid σ-θ levels, the definition of the model levels changes with altitude. Above a reference potential temperature, θ_0, the model uses pure isentropic levels and the potential temperature of an interface is defined as

$$\theta_{k+\frac{1}{2}} = C\theta_0 \quad (C \geq 1). \tag{2}$$

Between θ_0 (e.g. typically 350 K) and the surface, the model uses hybrid levels. The pressure of the model half-levels in this region is then given by

$$p_{k+\frac{1}{2}} = Cp_{\theta 0} + (1 - C)p_s \quad (C < 1), \tag{3}$$

where $p_{\theta 0}(\lambda, \phi)$ is the pressure at the lowest purely isentropic half-level. This method of defining a vertical coordinate is possible in an off-line CTM as p at the surface, p_s, and at θ_0 are known at future times (using p_s and T from the analyses). This coordinate would likely not be straightforward in a GCM where both p_s and T are prognostic variables. Alternative definitions of the hybrid σ-θ based on θ at the surface were tested. However, stable temperature profiles in the troposphere led to model levels which contained very little mass which could result in the tracer advection becoming unstable. The adopted definition involving pressure ensures a more even distribution of mass over all tropospheric layers.

(*c*) *Vertical transport*

Off-line CTMs either need to take the vertical wind from the forcing analyses or to diagnose this from the fields available. There are inherent problems in this, as discussed

in Jöckel *et al.* (2001) and Rotman *et al.* (2004), related to the use of meteorological fields with inconsistent winds and surface pressures. These problems can be related to the time discretization of the archived fields or due to the regridding of the analyses from the GCM which provides the winds. These problems will generally not occur in on-line tracer advection within a GCM.

Most meteorological analyses archive the vertical wind and so taking this is an option. However, after interpolation from the analysis grid to the model grid, there may no longer be consistency between the horizontal and vertical winds. Also, if the model levels do not coincide with the analysis levels, some form of vertical interpolation is required, which is not desirable. Therefore, in TOMCAT/SLIMCAT the vertical motion is diagnosed from the fields available on the model grid. There are two options for doing this.

The first option is to diagnose the vertical mass fluxes from the horizontal mass fluxes using continuity. After the horizontal winds have been averaged onto the model grid (section 2(a)), the vertical mass flux, w_{m}, can be calculated from the divergence of the horizontal mass flux, D_{m}. For example, in pressure coordinates, w_{m} across surface p_k is calculated by

$$w_{\mathrm{m}} = \int_{p=0}^{p=p_k} D_{\mathrm{m}}\, \mathrm{d}\eta.$$

This uses the boundary condition that $w_{\mathrm{m}} = 0$ at $p = 0$ and ensures consistency between the horizontal and vertical mass fluxes. In hybrid σ-p coordinates, a correction needs to be added to take account of the change in vertical coordinate (calculated from $\mathrm{d}p_{\mathrm{s}}/\mathrm{d}t$ and vertical coordinate parameter B). When using mass flux divergence in hybrid σ-θ coordinates, a different approach is used as the time rate of change of model level pressure is not known from information at a single analysis time. In this coordinate the calculation again starts with the equation

$$w_{\mathrm{m}} = w_{\mathrm{m0}} + \int_{p=p_{\mathrm{top}}}^{p=p_\theta} D_{\mathrm{m}}\, \mathrm{d}\eta,$$

where p_{top} is the pressure of the upper interface of the top model θ level (which is not 0), w_{m0} is the vertical mass flux into this top level (obtained from the analyses), and p_θ is the pressure of the model θ level at the current time t. The correction needed due to the change in model interface pressure is obtained by using the analyses at $t + 6$ hours and simply estimating $\mathrm{d}p/\mathrm{d}t$ from this difference.

A second option for calculating the vertical transport in the θ-coordinate domain of the σ-θ model is to use calculated heating rates. This was the default method in past studies with the pure θ-coordinate version of SLIMCAT (e.g. Chipperfield 1999). In this method the net diabatic heating rate, Q, is converted to a vertical mass flux:

$$w_{\mathrm{m}} = -Q\left(\frac{p_o}{p}\right)^{\kappa} \frac{1}{g}\frac{\mathrm{d}p}{\mathrm{d}\theta}.$$

Within TOMCAT/SLIMCAT, Q is calculated using a radiation scheme (see section 2(d)). With this method, as implemented in TOMCAT/SLIMCAT, there is no forced balance between horizontal and vertical mass fluxes. Weaver *et al.* (2000) developed a θ-coordinate model and implemented a procedure which ensured consistency between the vertical motion diagnosed from a radiation scheme and the horizontal winds. They did this by combining the divergence of the calculated vertical winds with the vorticity from the analyses to recalculate the horizontal wind field.

TABLE 1. DETAILS OF CTM RADIATION SCHEMES

	MIDRAD	CCMRAD
Temperature	Analyses	Analyses
Domain	0–700 hPa	0 hPa–surface
Long wave	CO_2 15 μm O_3 9.6 μm vibro bands H_2O	O_3, CO_2, H_2O, CH_4, N_2O, F11, F12 0–3000 cm^{-1} $\Delta\lambda$ 100 cm^{-1}
Short wave	O_2 and O_3 6 bands 125–175, 175–205 nm, 206–244, 244–278 nm, 278–363, 408–853 nm	O_2, O_3, CO_2, H_2O 18 intervals 200–5000 nm
Albedo	0.2 ($\lambda_w > 278$ nm)	Climatology fn(λ_w, t, ϕ)
Clouds	None	Not included here
References	Shine (1987) Shine and Rickaby (1989)	Briegleb (1992)

(*d*) *Radiation schemes*

Two different radiation schemes are included in the model for the calculation of vertical transport in isentropic coordinates. The default scheme in past SLIMCAT studies was the relatively simple MIDRAD scheme (Shine 1987). Recently we have added a more sophisticated scheme, used in a GCM and here called CCMRAD (Briegleb 1992), to investigate how this affects the model. Table 1 summarizes details of these two schemes. It should be noted that neither of these schemes is used in the meteorological models which produce the analyses used to force the model, although the CCM scheme is most similar in terms of complexity. Ideally, an off-line model would use the same radiation scheme as the 'on-line' model for consistency. Even then, for an exact recalculation of heating rates, one would still need all the necessary forcing fields including, for example, cloud information. This probably makes more difference than the choice of radiation scheme. We have done tests with a version of the Morcrette scheme (W. Zhong 2002, personal communication), based on that used in the ECMWF model, but with just temperature taken from the analyses. For this we find results similar to the CCM scheme.

(*e*) *Mass balance in heating rates*

In the atmosphere the vertical mass flux between $\phi = \pm\pi/2$ and $\lambda = \pm\pi$ must be zero when integrated over a pressure surface. An equivalent condition is that the area-averaged vertical velocity must be zero, i.e.

$$\int_{-\pi}^{\pi}\int_{-\pi/2}^{\pi/2} w\cos\phi\,\mathrm{d}\phi\,\mathrm{d}\lambda = 0.$$

As emphasized by Shine (1989), this condition does not mean that the global net mean heating rate be zero when averaged on an isobaric surface. The actual condition for Q is

$$\int_{-\pi}^{\pi}\int_{-\pi/2}^{\pi/2}\left(Q - \frac{\partial\theta}{\partial t} - \frac{1}{a}\mathbf{v}\cdot\nabla\theta\right)\left(\frac{\partial\theta}{\partial z}\right)^{-1}\cos\phi\,\mathrm{d}\phi\,\mathrm{d}\lambda = 0.$$

On an isentropic level this simplifies to

$$\int_{-\pi}^{\pi}\int_{-\pi/2}^{\pi/2} Q\left(\frac{\mathrm{d}\theta}{\mathrm{d}z}\right)^{-1}\cos\phi\,\mathrm{d}\phi\,\mathrm{d}\lambda = 0. \tag{4}$$

Therefore, in the hybrid σ-θ level model (SLIMCAT), the mass balance (Eq. (4)) is applied to the pure θ levels above 380 K. This is done at the time of diagnosing the heating rates and, in addition to the general issues of 3D model mass balance, is related to the vertical coordinate and temporal discretization discussed in section 4 below. The need for this correction to Q points towards deficiencies in the radiation schemes used or an inconsistency in the temperature and radiatively active tracer fields used. (Note that in a GCM such deficiencies in the radiation scheme would lead to erroneous temperature fields.) Below 380 K, where the model levels will intersect the troposphere in any case, the calculated heating rates (used down to θ_0) are not adjusted. Below θ_0 vertical motion is always taken from the analyses.

(*f*) *Advection schemes*

The quality and properties of the tracer advection scheme have a large influence on the success of CTM simulations. Unfortunately, no single advection scheme has all of the desired properties of conservation, monotonicity, low numerical diffusion and low dispersion. Therefore, a compromise is necessary when selecting a scheme. Within a CTM, another important consideration is that the advection scheme should preserve tracer–tracer correlations and total family abundances, i.e. the advection should not be tracer-specific. This usually rules out the use of tracer-specific 'flux correctors' or 'limiters'. The two principal advection schemes used in TOMCAT/SLIMCAT are now described.

(i) *Prather scheme.* The default advection scheme in the model is the conservation of second-order moments scheme described by Prather (1986). This Eulerian finite volume is used separately for advection in the x, y and z directions based on mass fluxes averaged over the interfaces of the model grid. The scheme has the desirable properties of exact mass conservation and low numerical diffusion. However, it is not monotonic and care has to be taken if dealing with overshoots or undershoots in multi-tracer runs that tracer–tracer correlations are not affected. The scheme can also be used with the conservation of first-order moments which is computationally cheaper and is equivalent to the slopes scheme of Russell and Lerner (1981).

(ii) *Semi-Lagrangian scheme.* We have also implemented a semi-Lagrangian transport (SLT) advection scheme in TOMCAT/SLIMCAT. SLT schemes have been popular in atmospheric models and offer some advantages over other (Eulerian) advection schemes. SLT schemes are not limited by the Courant–Friedrichs–Lewy condition and so can be used in high-resolution models without the need for a very short time step. Part of the cost of SLT schemes is the calculation of the back trajectories. As this is done only once, SLT schemes become relatively cheaper for large numbers of tracers which may be used in full chemistry models. The principal problem with many SLT schemes used up to now (including the one presented here) is that they are non-conservative. These features are discussed in more detail by Staniforth and Coté (1991).

The semi-Lagrangian advection scheme implemented in the TOMCAT/ SLIMCAT CTM is based on the method of Williamson and Rasch (1989). It is similar to the advection scheme used in the REPROBUS chemical transport model (Lefèvre *et al.* 1994) and the former NCAR Community Climate Model (CCM2) (Hack *et al.* 1993). Tracers and winds are obtained on the trajectory positions using cubic interpolation.

(*g*) *Trajectories*

This new version of TOMCAT/SLIMCAT includes a module for the calculation of an arbitrary number of Lagrangian air mass trajectories. This module uses the same

wind fields as the rest of the CTM (interpolated to the individual trajectories) and the same options used for vertical coordinate and method of calculating vertical velocities. The trajectories are stepped forward over the basic CTM time step using a fourth-order Runge–Kutta time scheme (see Fisher *et al.* 1993). The inclusion of trajectories allows a Eulerian/Lagrangian comparison of transport within the same model run. The trajectory code is also used for the calculation of nitric acid trihydrate particle sedimentation in stratospheric full chemistry simulations which use the DLAPSE denitrification model (e.g. Mann *et al*. 2002).

(*h*) *Tropospheric physics*

The CTM contains a range of parametrizations to account for subgrid-scale transport in the troposphere.

(i) *Moist convection.* The CTM has the option of including a parametrization of moist convection based on the mass flux scheme of Tiedtke (1989). The implementation of this scheme in this new version of TOMCAT/SLIMCAT is essentially as described by Stockwell and Chipperfield (1999).

(ii) *Boundary layer.* The CTM has the option of parametrizing the vertical turbulent mixing, for example in the planetary boundary layer (PBL), either by the method of Louis (1979) or Holtslag and Boville (1993). The Louis (1979) scheme is a local first-order approach where the diffusion coefficient is calculated from the Richardson number. The Holtslag and Boville (1993) parametrization is a non-local scheme which also accounts for countergradient transport. The implementation of the Holtslag and Boville (1993) scheme in a similar CTM, and comparisons with the Louis (1979) scheme, are given in Wang *et al.* (1999). Based on ECMWF-forced TOMCAT runs, we find that the non-local scheme gives much stronger transport out of the PBL and tropospheric tracer distributions which agree better with observations.

(iii) *Simple mixing.* In addition to the more detailed tropospheric parametrizations described above, the model also includes the alternative of a simple, computationally cheap scheme to mix tracers vertically throughout the depth of the troposphere. This scheme is useful, for example, for long 'stratospheric' simulations where only long-lived source gases (e.g. N_2O, CH_4, certain halocarbons) are emitted and where the representation of the weak gradients in the troposphere are not important. When this scheme is used, all tracers in the troposphere are mixed over a column to achieve a constant mixing ratio profile over all model levels in that column which are contained completely within the troposphere (defined as potential vorticity < 2 SI units and $\theta <$ 380 K).

(*i*) *Chemistry*

The CTM includes two detailed chemistry schemes. One is the stratospheric scheme described by Chipperfield (1999) and previously used in many SLIMCAT (and early TOMCAT) studies. The CTM also contains a tropospheric scheme based on the ASAD code (e.g. see Law *et al.* 1998). As neither scheme is used in the simple tracer runs performed in this study, no further details are given here.

3. Model experiments

We have investigated the performance of the new CTM in different configurations by running a series of experiments to study stratospheric tracer transport.

TABLE 2. 3D CTM EXPERIMENTS

Experiment	Vertical coordinate	Vertical motion	Advection scheme	Winds	Resolution
UNI001	TOMCAT (σ-p)	Divergence	Prather	ECMWF	5.6° × 7.5° L24
UNI001_HI	TOMCAT (σ-p)	Divergence	Prather	ECMWF	2.8° × 3.75° L24
UNI001_L48	TOMCAT (σ-p)	Divergence	Prather	ECMWF	5.6° × 7.5° L48
UNI002	TOMCAT (σ-p)	Divergence	SLT	ECMWF	5.6° × 7.5° L24
UNI002_HI	TOMCAT (σ-p)	Divergence	SLT	ECMWF	2.8° × 3.75° L24
UNI002_L48	TOMCAT (σ-p)	Divergence	SLT	ECMWF	5.6° × 7.5° L48
UNI003	SLIMCAT (σ-θ)	Divergence	Prather	ECMWF	5.6° × 7.5° L24
UNI003_L48	SLIMCAT (σ-θ)	Divergence	Prather	ECMWF	5.6° × 7.5° L48
UNI004	SLIMCAT (σ-θ)	Divergence	SLT	ECMWF	5.6° × 7.5° L24
UNI005	SLIMCAT (σ-θ)	Heating (MIDRAD)	Prather	ECMWF	5.6° × 7.5° L24
UNI006	SLIMCAT (σ-θ)	Heating (CCMRAD)	Prather	ECMWF	5.6° × 7.5° L24
UNI007	SLIMCAT (σ-θ)	Heating (MIDRAD)	SLT	ECMWF	5.6° × 7.5° L24
UNI101	TOMCAT (σ-p)	Divergence	Prather	UKMO	5.6° × 7.5° L24
UNI105	SLIMCAT (σ-θ)	Heating (MIDRAD)	Prather	UKMO	5.6° × 7.5° L24

The model was run at a horizontal resolution of 5.6° latitude × 7.5° longitude. Although this is relatively coarse, it does allow a large number of decadal sensitivity tests. The model had 24 levels from the surface to ∼60 km.

The model runs included four idealized tracers to test the model transport. A tracer ('age tracer') with a linearly increasing surface mixing ratio was used to diagnose the stratospheric age of air. A further two tracers ('sin tracer' and 'cos tracer') had sinusoidally varying boundary conditions (period 1 year) in the tropical UT to diagnose the 'tape recorder'. Finally, the runs contained an idealized N_2O-like tracer with a tropospheric source and a stratospheric sink which increases with altitude. For this (N_2O-like) tracer, the assumed chemical lifetime (in days) was set equal to 10 × the local pressure (in hPa).

The model was forced using either UKMO (Swinbank and O'Neill 1994) or ECMWF ERA-40 (Uppala *et al.* 2004) analyses. All the model runs started with a nominal calendar date of 1 January 1983 and were integrated for 20 years. However, for the first 10 years the runs used the same annual (1992) forcing meteorology. After the model year 1992, the interannually varying meteorology was used up to 2001, after which 2001 was used perpetually. This was chosen because 1992 is the first full year of UKMO analyses available. Two runs were extended through to the nominal date of 2005 (with perpetual 2001 forcing) in order to compare ERA-40 winds with the operational winds of 2001. All model runs shown here used the 'simple mixing' tropospheric scheme (see section 2(h)(iii)).

The model experiments are summarized in Table 2. In total, nine basic model experiments were performed with different configurations or forcing winds. These experiments varied the model vertical grid, the method of calculating the vertical velocities in the stratosphere (i.e. above θ_0), the radiation scheme used to diagnose heating rates, and the advection scheme. A further five experiments were performed as variations of run UNI001, UNI002 and UNI003 but with double the horizontal resolution (UNI001_HI, UNI002_HI) or double the vertical resolution (UNI001_L48, UNI002_L48, UNI003_L48).

The basic model runs used 24 levels either defined as σ-p or σ-θ (see Eqs. (1)–(3)). The parameters used to define these levels are given in Table 3 and the mean pressure of the level centres for the two vertical coordinates are shown in Fig. 1. The levels were chosen so that the vertical resolutions of the two grids were similar and so that the highest vertical resolution is in the low/mid stratosphere.

TABLE 3. DEFINITION OF MODEL LEVELS

Interface	*A*	*B*	*C*
0	0	0	8.571428
1	0.000182	0	7.352018
2	0.000311	0	6.306086
3	0.000532	0	5.408953
4	0.000910	0	4.639451
5	0.001558	0	3.979421
6	0.002668	0	3.413291
7	0.004566	0	2.927700
8	0.007817	0	2.511192
9	0.013380	0	2.153938
10	0.017506	0	1.994849
11	0.022904	0	1.847509
12	0.029966	0	1.711052
13	0.039206	0	1.584674
14	0.051295	0	1.467630
15	0.067112	0	1.359231
16	0.087344	0.000461	1.258838
17	0.113065	0.001815	1.165861
18	0.139160	0.011143	1.079750
19	0.162527	0.034121	1
20	0.200486	0.099675	0.871149
21	0.182659	0.243933	0.713769
22	0.147052	0.433963	0.521546
23	0.086359	0.683269	0.286764
24	0.000000	1	0

See Eqs. (1), (2) and (3).

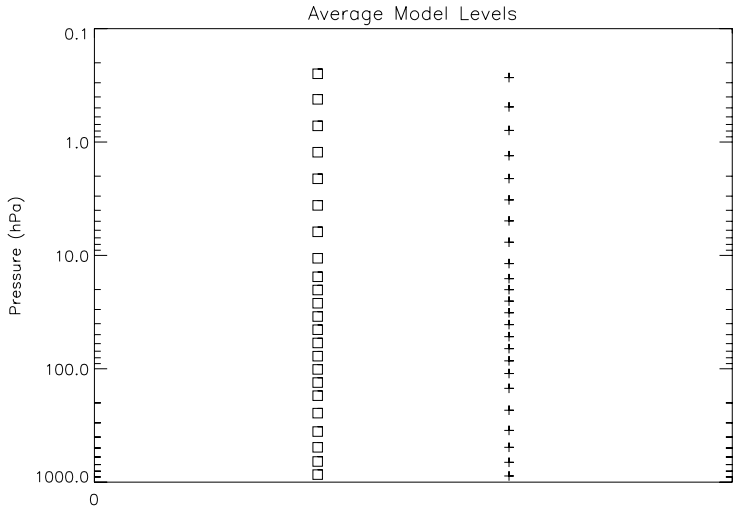

Figure 1. Mean pressure (hPa) of model centre-levels for the tracer experiments used in this study (see parameters in Table 3) for the 24 hybrid σ-p level runs (□) and the 24 hybrid σ-θ level runs (+). The pressures are annual means calculated using ECMWF 1992 meteorology.

4. MASS BALANCE

The accurate conservation of tracer mass is a desirable property of all atmospheric models. However, there are many factors which may prevent this conservation over all possible scales. Off-line models also have certain specific problems.

A prerequisite for mass conservation in a CTM is that the chemistry scheme conserves mass (or atoms). That should be straightforward to achieve with all useful

chemical integrators. Another essential element is that the model's advection scheme conserves mass. Of the two schemes contained in TOMCAT/SLIMCAT and described here, the Prather scheme (and variations) does conserve mass. However, the SLT scheme, which deals with the volume mixing ratios of tracers on trajectories, does not.

However, a more difficult issue for mass conservation in a CTM concerns the balance of mass transported between grid boxes, and the predicted mass of that grid box based on the evolving meteorological analysis fields. At a given instant, for which analysis fields are available, it will be possible for the net mass transport into a box to balance the mass tendency of that box, but the net effect of this transport over one meteorological cycle (e.g. 6 hours between the available analyses) cannot be guaranteed to balance.

The simplest case to consider is σ-p coordinates with the vertical mass flux calculated from the divergence of the horizontal mass fluxes (e.g. as in the TOMCAT model). In pure p coordinates, the mass of a grid box does not vary with time. Therefore, so long as the net mass flux into a box is zero at all times, the mass of the box will always be equal to that expected. In the hybrid σ-p domain, the mass of the box will vary with time as p_s varies. At the times where the (instantaneous) meteorological fields are available, and both p_s and $\mathrm{d}p_s/\mathrm{d}t$ are known, the instantaneous net mass fluxes can balance the rate of change of grid-box mass. However, a problem arises because of the lack of information between analysis times. In TOMCAT/SLIMCAT, meteorological fields are interpolated linearly in time to intermediate time steps (typically 30 minutes). Although the tracer advection scheme may conserve mass globally, there is no guarantee that locally the actual box mass after 6 hours advection equals that predicted by the new p_s value. This is the nature of the mass correction that is applied in TOMCAT (Stockwell and Chipperfield 1999). Figure 2(a) shows the calculated difference in mass after one time step in run UNI001. As expected, there is no mass difference in the pure p domain above 67 hPa. Below this there are differences of up to 1.5% in the zonal mean. Figure 2(b) shows the accumulated local change after 10 days. The accumulated total correction (applied in small increments every 6 hours) can reach 37% of the actual mass near the poles.

The mass balance problems are compounded in θ coordinates. Here the mass of grid boxes will also change with time, but unlike in σ coordinates, the tendency of the grid-box mass cannot be calculated using the meteorological fields routinely available (i.e. one would need to know $\mathrm{d}T/\mathrm{d}t$—the net heating rate—which is not always archived). Therefore, in the σ-θ version of SLIMCAT, the vertical mass fluxes are calculated at each analysis time assuming a fixed grid-box mass. A correction is then needed to account for the change in box mass with time. This is obtained in a general way (i.e. independent of the type of model vertical coordinate) from the calculated change in box mass over the next meteorological cycle (e.g. 6 hours), based on the mass diagnosed by the $t + 6$ hours analyses. This mass change, i.e. the movement of the model interface in θ coordinates, is converted to a correction to the vertical mass flux which is applied every time step over this meteorological cycle. Figure 2(c, d) shows the magnitude of this mass correction for SLIMCAT with the vertical motion diagnosed from divergence (i.e. being consistent with the horizontal winds). The corrections are now non-zero in the stratospheric θ coordinates. (Note that the large changes near the top level are because the total model domain no longer extends to 0 hPa). Finally, Fig. 2(e, f) shows the same mass corrections in SLIMCAT when the vertical motion is diagnosed from heating rates in the stratosphere. Over one time step, local zonal mean differences are typically around 0.2% and the accumulated local change after 10 days is largely around 10%, though some regions with much larger changes (e.g. the tropical UT) exist.

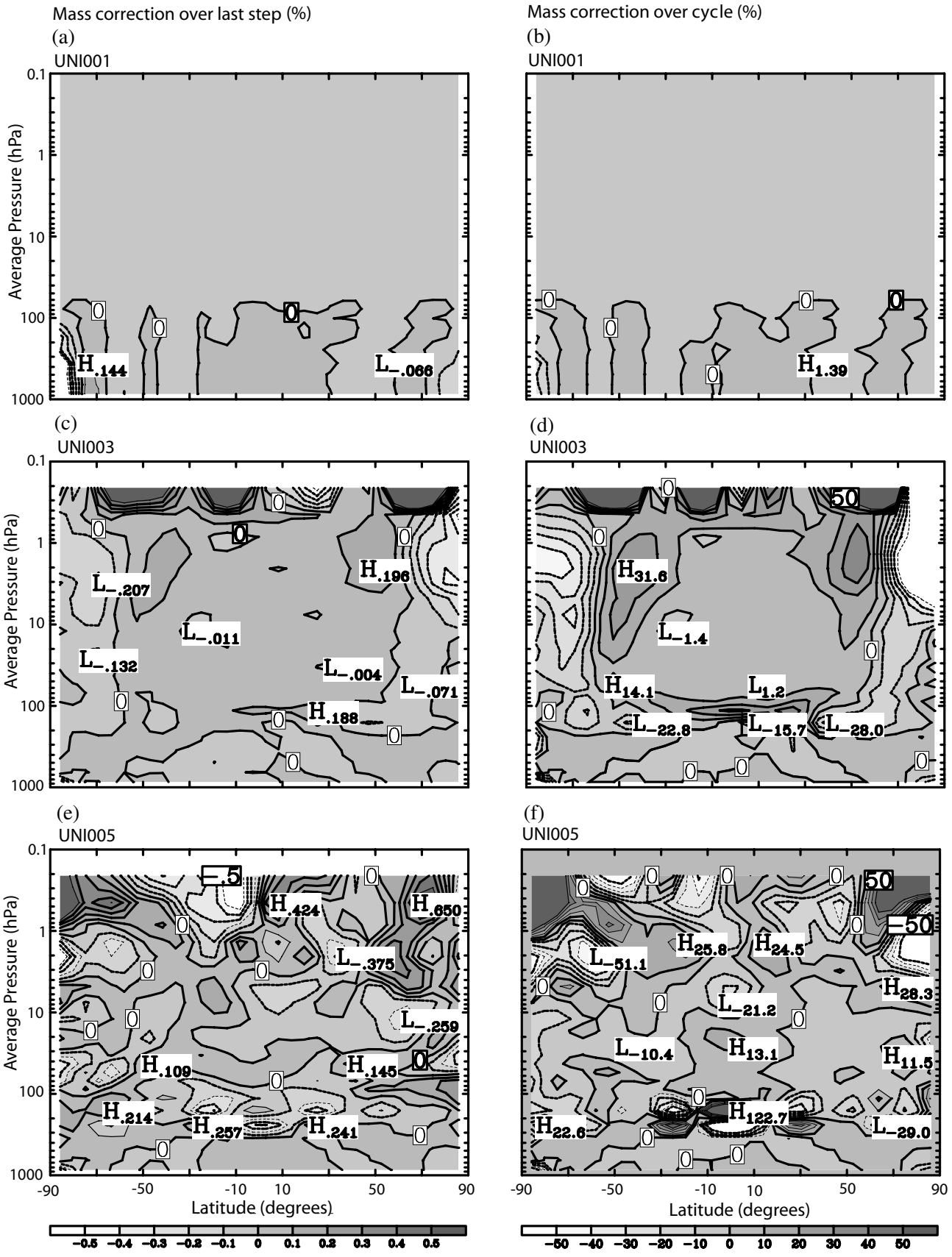

Figure 2. Annual average zonal mean latitude–height plots of the mass correction (%) for (a) one model time step (contour interval 0.1), and (b) 10 days (contour interval 10) for run UNI001. (c, d) and (e, f) are as (a, b) but for runs UNI003 and UNI005, respectively.

This discussion on mass balance is included here in order to explain the formulation of the CTM and to illustrate the magnitude of the mass correction employed. However, it should be noted that many CTMs seem to give reasonable simulations without concern over mass conservation in advection schemes or the balance of winds. In the case of the default σ-θ SLIMCAT model (i.e. run UNI005 using diagnosed heating rates for the vertical motion), it still performs well in reproducing the main features of stratospheric chemistry over decadal time-scales (e.g. Chipperfield 2003).

The various aspects of mass conservation in off-line (and on-line) models should be remembered when defining experiments. There will be situations in which exact mass conservation is a necessity, in which case a p-coordinate model would be used, despite it likely giving a poorer circulation (see below). Alternatively, to obtain the most realistic tracer distributions, e.g. for a chemical sensitivity experiment, then a θ-coordinate model can be used. However, the magnitude of the (unavoidable) mass correction should be considered when analysing the results.

5. Results

(*a*) *Age of air*

First we look at the age of air calculated in the different experiments. Age of air has become a useful diagnostic of stratospheric transport, although values inferred from observations are limited. The concept is discussed in Hall *et al.* (1999) and was first used to show that many models (mainly 2D) gave ages of air in the stratosphere which were much too low.

Eluszkiewicz *et al.* (2000) investigated the sensitivity of modelled age of air to the choice of advection scheme in a 3D GCM. They found a large sensitivity of the modelled age, with a less diffusive (centred-difference) advection scheme giving a much greater age than a diffusive SLT scheme. Their SLT scheme, like TOMCAT/SLIMCAT, was based on Williamson and Rasch (1989) but with monotonicity imposed, which makes it more diffusive. Also, their 'less diffusive' scheme will likely still be more diffusive than the Prather (1986) second-order moments scheme. The full reasons for this difference in Eluszkiewicz *et al.* (2000) were not clear, but they suggested that part of the problem was short-term variability on the time-scale of their model's 3-minute advection step. A similar SLT advection scheme, but with a much longer time step, in a different GCM gave a much greater age, indicating the large numerical diffusion which can result from tracer interpolation in a SLT scheme. Eluszkiewicz *et al.* (2000) noted that for slow, smoothly varying circulations, as produced by 2D latitude–height models, the calculated age is insensitive to the advection scheme.

Here we investigate the sensitivity of the modelled age of air to the choice of model vertical coordinate, method of calculating the vertical motion, resolution, choice of winds and advection scheme. Many of these tests are performed using constant 1992 meteorology (the first full year for which we have both ECMWF and UKMO analyses). We also investigate the effect of meteorological variability on the modelled age of air.

(i) *Perpetual 1992 analyses.* Figure 3 shows latitude–height plots of the zonal mean annual mean age of air for 1992 from nine basic model simulations. There are significant differences between the different simulations. Figure 3(a) can be considered the basic 'TOMCAT' simulation which uses σ-p levels, the Prather (1986) advection scheme and vertical winds derived from divergence. The calculated age of air in the upper stratosphere (US) is only $\sim$2.5 years or so. Compared with this run, changing the vertical coordinate to stratospheric θ levels has a quite dramatic effect on the modelled age of

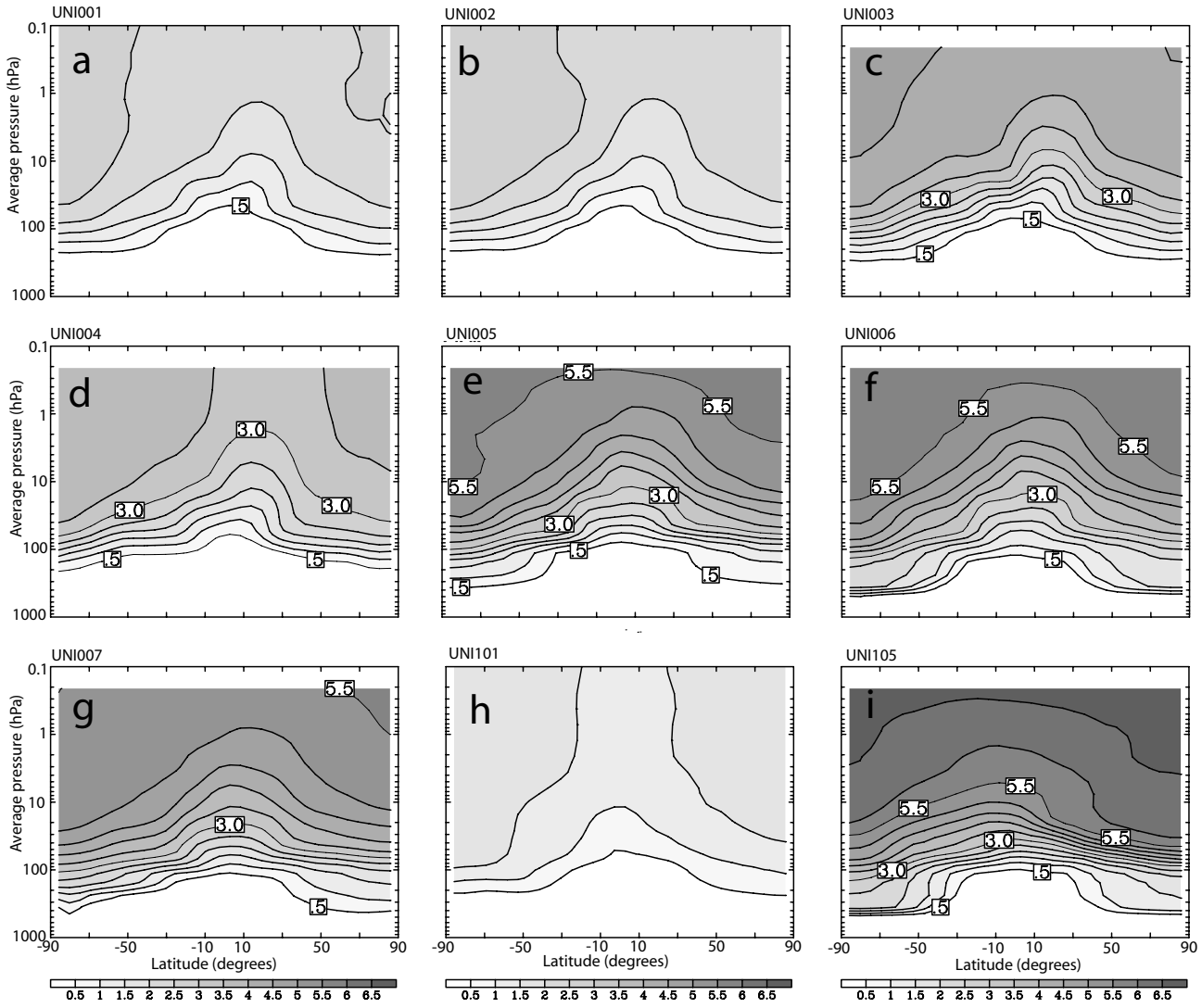

Figure 3. Latitude–height plots of the annual mean zonal mean age of air for model year 1992 (i.e. after 10 years of repeating 1992 meteorology) for a series of model runs with a horizontal resolution of 5° × 7.5°: (a) UNI001, (b) UNI002, (c) UNI003, (d) UNI004, (e) UNI005, (f) UNI006, (g) UNI007, (h) UNI101, and (i) UNI105. The contour interval is 0.5 years.

air (Fig. 3(c); run UNI003) with ages in the US of ∼4.5 years. Relative to this run, the stratospheric age of air is increased further to ∼5.5 years if we use a radiation scheme to calculate the vertical motion in θ coordinates (Figs. 3(e) and (f); runs UNI005, UNI006). The CCMRAD radiation gives a slightly greater age of air than the MIDRAD scheme, especially in the high-latitude LS. Changing from the Prather (1986) advection scheme to the SLT scheme results in lower ages of air for all variations of the model, e.g. pressure level (Fig. 3(a) versus 3(b)) and the θ level model (Fig. 3(c) versus 3(d) and Fig. 3(e) versus 3(g)). Finally, changing from ERA-40 re-analyses (UNI001) to UKMO analyses (UNI101) produces an even lower age of air for the p-coordinate model but a greater age of air for the θ level model. (The use of the divergence to calculate the vertical winds in run UNI101 is particularly problematic as this needs to be recalculated from the available grid-point u and v which have already been interpolated onto the UARS levels. Early tests with this model set-up in 1995 was the motivation for creating SLIMCAT from TOMCAT.)

The differences in the modelled age of air in Fig. 3 follow the pattern that the more diffusive SLT advection scheme gives a lower age of air than the Prather (1986) scheme, p levels give a lower age of air than θ levels, and analysed winds give a lower age of

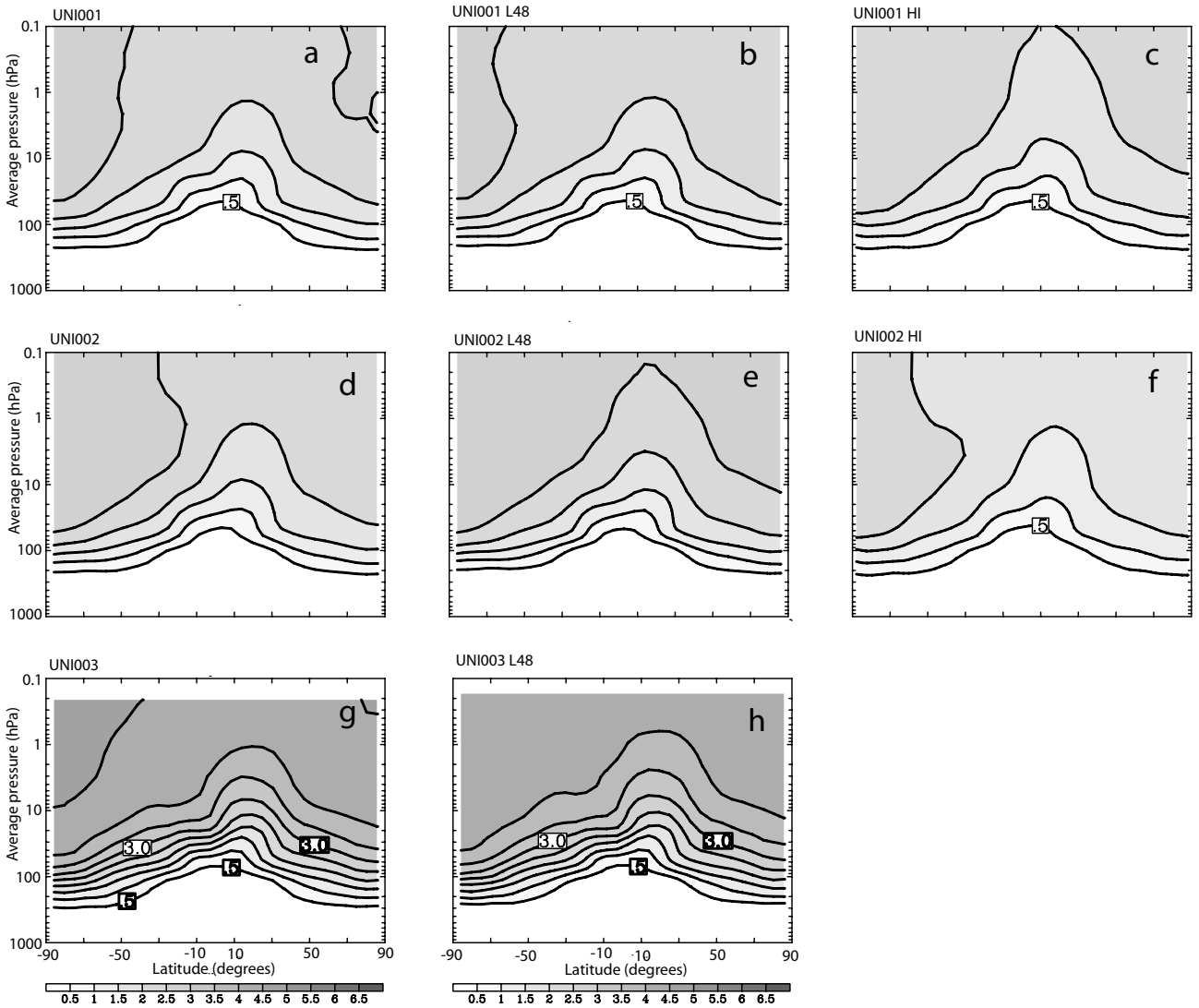

Figure 4. As Fig. 3, but comparing basic model runs with equivalent simulations at higher horizontal or vertical resolution: (a) UNI001, (b) UNI001_L48, (c) UNI001_HI, (d) UNI002, (e) UNI002_L48, (f) UNI002_HI, (e) UNI003, and (f) UNI003_L48. (a), (d) and (g) are repeated from Fig. 3(a), (b) and (c) for clarity.

air than diagnosed heating rates. The greater age of air in the polar LS produced by the CCMRAD scheme helps explain the improvements in the simulated springtime O_3 loss in this version of SLIMCAT (see Feng *et al.* 2005). Schoeberl *et al.* (2003) compared age of air simulations using a trajectory model and a 3D CTM forced by both analyses and GCM winds. They found that the analyses tested, including UKMO, produced too much mixing between the tropics and extratropics. Figure 3 shows different tracer gradients in the subtropics with different model formulation and with different analyses. The ERA-40 winds tend to give stronger subtropical gradients than the equivalent UKMO simulations.

Figure 4 compares the modelled age of air for three of the runs shown in Fig. 3 with equivalent runs with double the vertical resolution. Comparing Figs. 4(d) and (e) shows that the SLT advection scheme increasing the vertical resolution leads to an increase in the modelled age of air in the US. In the SLT scheme, the model vertical winds are first obtained on the ECMWF 60 analysis levels and then interpolated onto the back trajectories. Changing the vertical resolution cannot, therefore, change the vertical motion of the back trajectories but does decrease the numerical diffusion of the interpolation scheme. In contrast, increasing the vertical resolution of the runs using

the Prather advection scheme (Fig. 4(a) versus (b); Fig. 4(g) versus (h)) has very little effect, except in the US. The model is formulated so that, with such an advection scheme, the vertical mass fluxes (integrated from the analyses) are independent of the vertical resolution. This accounts for the only small changes but it is somewhat counter-intuitive that the higher-resolution model, with less numerical diffusion, has the lowest age in the US.

Figure 4 also shows the effect of doubled horizontal resolution of the modelled age of air for runs UNI001 and UNI002. In the LS, there is no apparent significant change in run UNI001. In the US, the higher-resolution run UNI001_HI has a lower age of air; there is a more isolated ascent of air masses in the tropics. For the more diffusive SLT scheme, the differences are more marked; there is now a difference in the LS as well as higher up, but the higher horizontal resolution leads to lower ages.

The above results show that, even when using the same wind fields, model formulation has an effect on the modelled age of air. In particular, the change in modelled age when changing the vertical coordinate can be dramatic. In general, increasing a model resolution will tend to decrease numerical diffusion, as tracers will not be artificially spread over as large a grid box. As shown in Fig. 4, the effect of a simple resolution change in TOMCAT/SLIMCAT is, depending on the advection scheme, quite small.

In the stratosphere, θ coordinates give a clearer separation between horizontal and vertical (diabatic) motion. However, when using p coordinates, rapid quasi-isentropic horizontal motion will cause tracers to be advected between model levels. This spurious vertical transport, due to horizontal advection on surfaces of constant p, will spread tracers too rapidly. The removal of this in θ coordinates is likely to be the cause of the large improvement in modelled age between runs UNI003 and UNI001. To verify this, a sensitivity test was done. Runs UNI001 and UNI003 were repeated but with only vertical advection (i.e. no horizontal transport). After 6 years of integration the modelled tracer fields, although unrealistic, were very similar between the model formulations, and did not show the large differences of Fig. 3 (not shown). These quasi-1D tests support the result that the choice of model grid is more important than a modest change in model resolution.

As different model formulations produce very different ages of air, it is important to assess which is more realistic. Figure 5 compares model-calculated age of air with *in situ* balloon and aircraft observations in the lower/mid stratosphere. At 20 km the observed mean age shows tropical values of around 1 year and large latitudinal gradients with high-latitude values near 5–6 years. The model runs which use σ-p levels and vertical motion from the divergence (runs UNI001 and UNI101) severely underestimate this gradient and have mean ages at high latitudes of only 1.5–2.5 years. These runs also underestimate the mean age in the range 20–30 km observed from balloons (Figs. 5(b)–(c)). Model run UNI003, which used the same vertical winds as run UNI001 but with σ-θ levels, does show an improvement. The mean age is around 3–4 years at high latitudes at 20 km and $\sim$4 years near 30 km in the profiles shown. This is near the lower estimates from the observations. The greatest, most realistic, ages are produced in the model version which uses both θ levels in the stratosphere and vertical motion from heating rates (runs UNI005 and UNI105). The results from these runs tend to span the observed values. Although results from the UKMO analyses (run UNI105) are sometimes about 2 years greater than ECMWF ERA-40 (run UNI005), a similar large difference occurs in the observations (e.g. 25–30 km at 40°N). The use of two different analyses, UKMO and ECMWF, has led to different modelled age of air. Although both analyses represent the same 1992 atmosphere, some differences are not unexpected and represent an uncertainty in the use of analyses for off-line modelling.

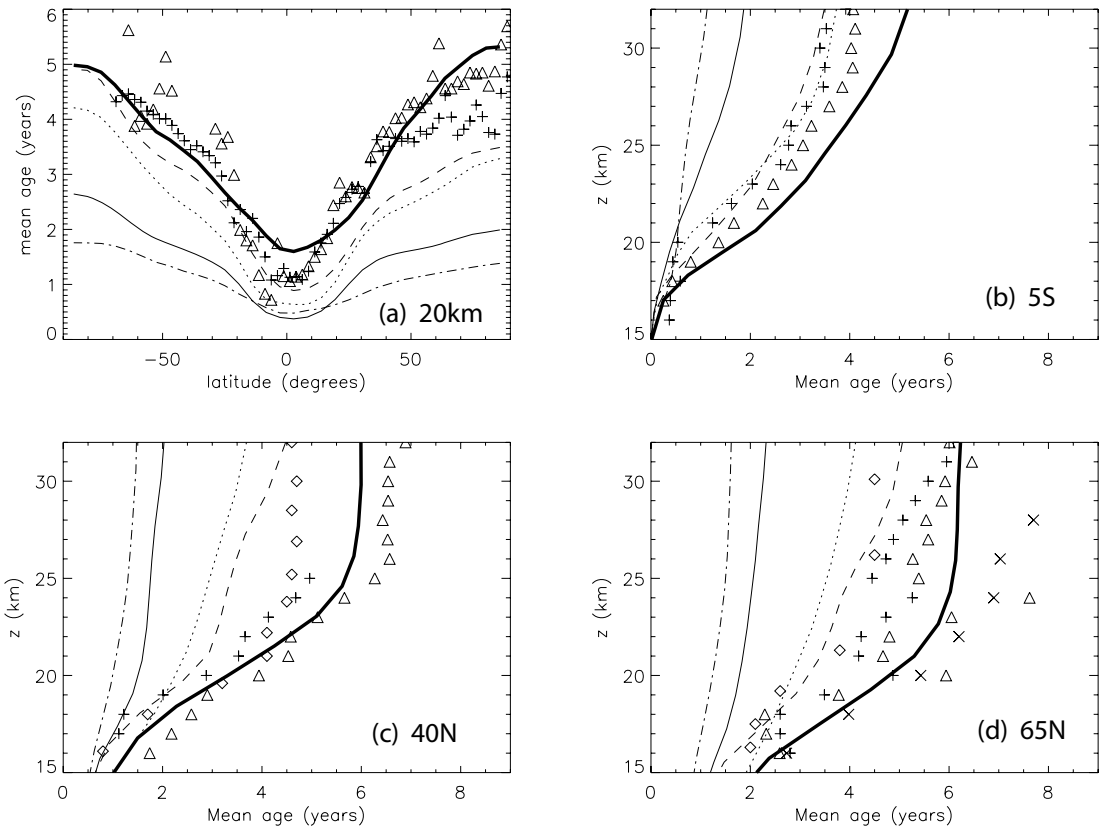

Figure 5. Mean age of air derived from observations (symbols) for (a) altitude 20 km and latitudes (b) 5°S, (c) 40°N, and (d) 65°N. Also shown (lines) are annual mean, zonal mean model results (for 1992) from CTM runs UNI001 (solid), UNI003 (dotted), UNI005 (dashed), UNI101 (dot-dashed) and UNI105 (bold solid). The symbols represent observations: mean age from *in situ* CO_2 (◇) (Boering *et al*. 1996; Andrews *et al*. 2001), *in situ* SF_6 (△) (Elkins *et al*. 1996; Ray *et al*. 1999), and whole air samples of SF_6 (+ outside vortex and × inside vortex) (Harnisch *et al*. 1996). Figure adapted from Waugh and Hall (2002).

However, issues related to the analyses themselves will contribute to this large (2-year) difference. First, the different analyses, produced at different resolution and with different schemes, should be compared with observations (e.g. temperature) to decide if one is a priori more realistic. Then, the method by which the analyses are used to force the off-line model should be considered. As stated above, the use of UKMO winds is hampered by the fact that they provide the horizontal wind components interpolated to 22 standard pressure levels.

(ii) *Interannual variability.* The discussion above focused on differences in model formulation based on simulations with perpetual 1992 forcing winds. The CTM simulations also allow us to investigate the effect of interannual meteorological variability on the age of air. Based on full chemistry model runs, such variability is known to be important in controlling, for example, interannual changes in high-latitude wintertime column ozone (e.g. Chipperfield and Jones 1999).

Figure 6 shows the modelled age of air from years 1992–2001 from two runs compared to the same observations in Fig. 5. For the profiles the modelled age generally varies by about 0.5 years, although for the more realistic run UNI005 the spread near 20 km can be ∼1 year. A similar spread of results is shown in the latitude cross-section. The observations do not really allow a separation of different years, but the model results indicate that this interannual variability might be seen in a larger dataset.

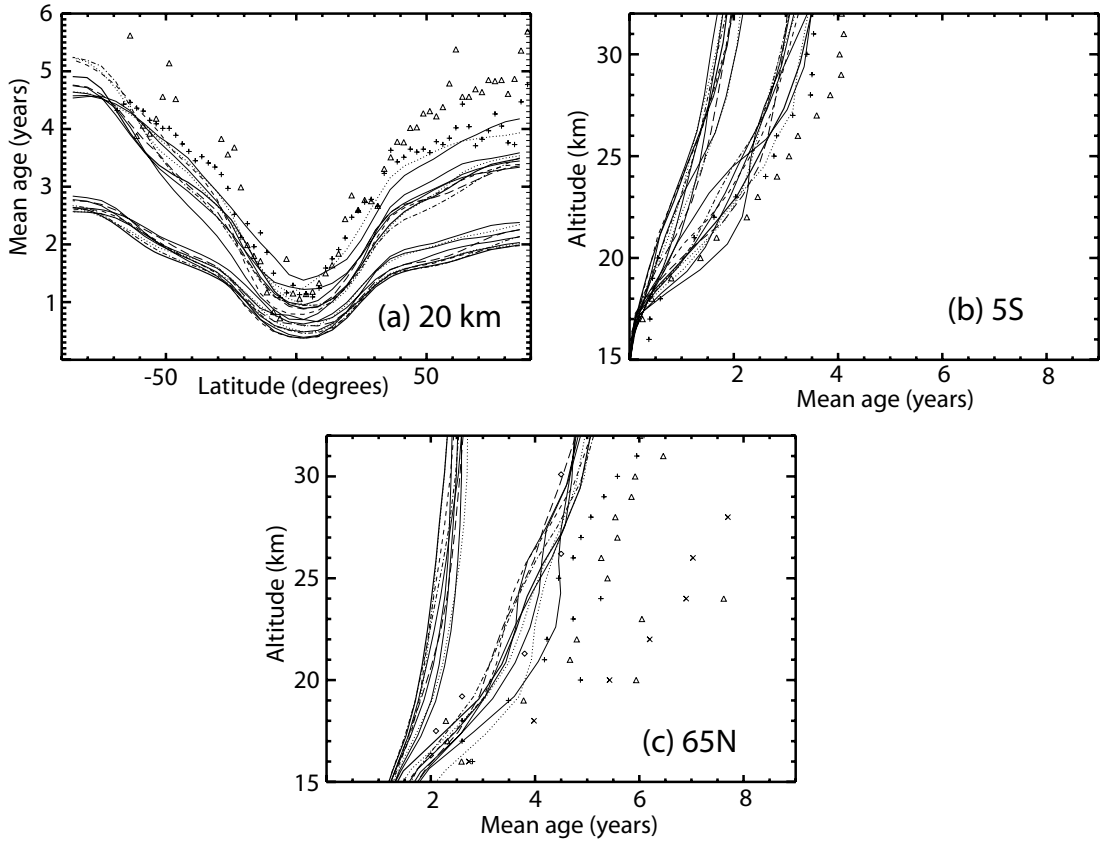

Figure 6. Mean age of air derived from observations (symbols) for (a) altitude 20 km and latitudes (b) 5°S and (c) 65°N. Also shown (lines) are annual mean, zonal mean model results for 10 years (1992–2001) from CTM runs UNI001 (low ages), and UNI005 (greater ages). The observations are the same as in Fig. 5 and the individual model years are not labelled.

Moreover, it shows that, when comparing model results, care should be taken to compare the same year for different models, or to allow for this variability by other methods.

(*b*) *Tape recorder*

The 'sin' and 'cos' tracers in the model allow us to investigate the tropical tape-recorder signal. Figure 7 shows the time evolution of the sin tracer in the tropics from model years 1991–2002 for four runs. In all cases the periodic boundary condition, applied at the lowest level in the tropics, can be seen. However, there is a difference in the rate at which this signal is propagated vertically. Following the repeated 1992 meteorology used until 1992, there is also interannual variability in this propagation.

Figure 8 compares profiles of the calculated phase and amplitude of the model tape-recorder signal (using the cos and sin tracers) from model runs UNI001, UNI003 and UNI005. Also shown are the calculated phase and amplitude from Halogen Occultation Experiment (HALOE) satellite and Observations of the Middle Statosphere (OMS) balloon observations. Note that the balloon data are much more sparse than the satellite data and that the diagnosed amplitude differs by a factor of three towards the upper limit of the balloon data (25 km). This may partly reflect interannual variability but it is likely that the satellite data provide the more reliable estimate of the mean amplitude here. Run UNI001 gives a phase which does not decrease strongly enough with altitude, i.e. the signal propagates too fast. The amplitude of the signal also decays more rapidly than the HALOE data, though it is still larger than the balloon signal which extends to 26 km. Model run UNI003 produces a slightly slower propagation of the phase,

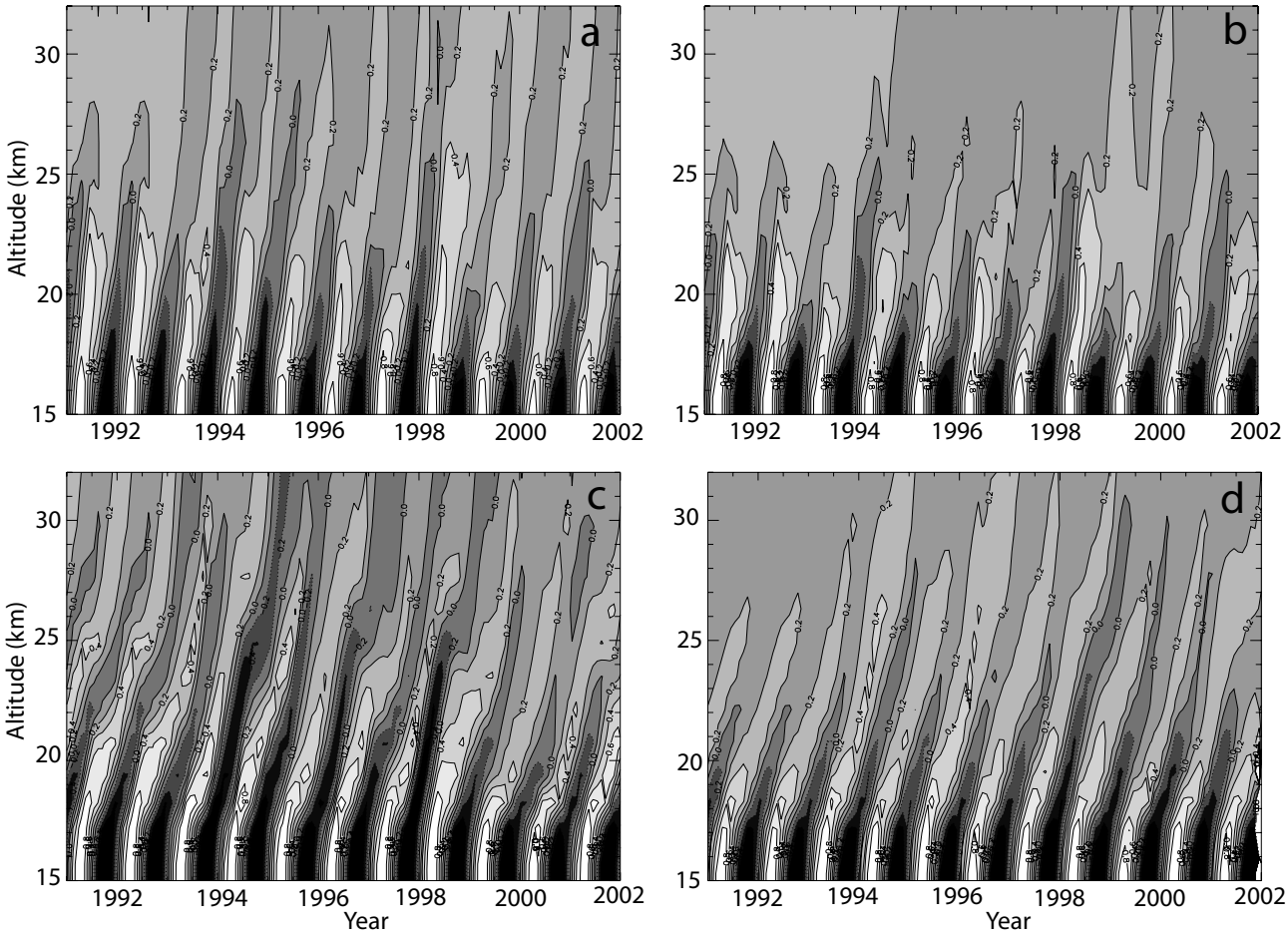

Figure 7. Height–time plots of model sin tracer for runs (a) UNI001, (b) UNI003, (c) UNI005, and (d) UNI105 for model years 1991–2002. The sin tracer is set to values varying between ±1 in the tropical troposphere with a period of 1 year. The contour interval is 0.2.

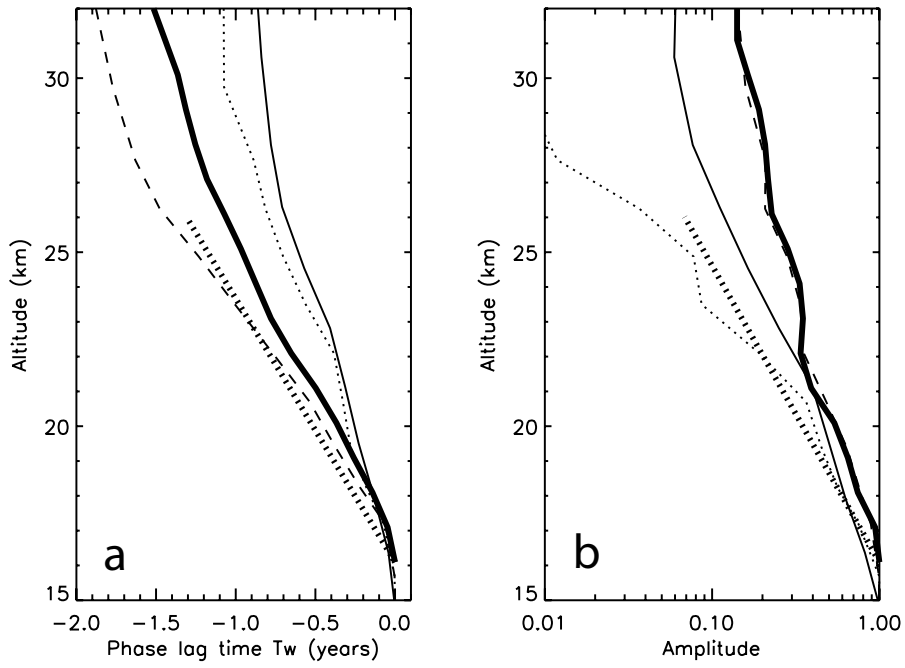

Figure 8. Height-resolved profiles of (a) the phase and (b) the amplitude of the model tape recorder at the equator for model years 1987–92 (i.e. perpetual 1992 forcing) for runs UNI001 (solid), UNI003 (dotted) and UNI005 (dashed). Also shown are amplitude and phase estimated from the HALOE $2CH_4 + H_2O$ data 1992–98 (bold solid) and from OMS balloon data (bold dotted). Data are from Norton and Iwi (1999).

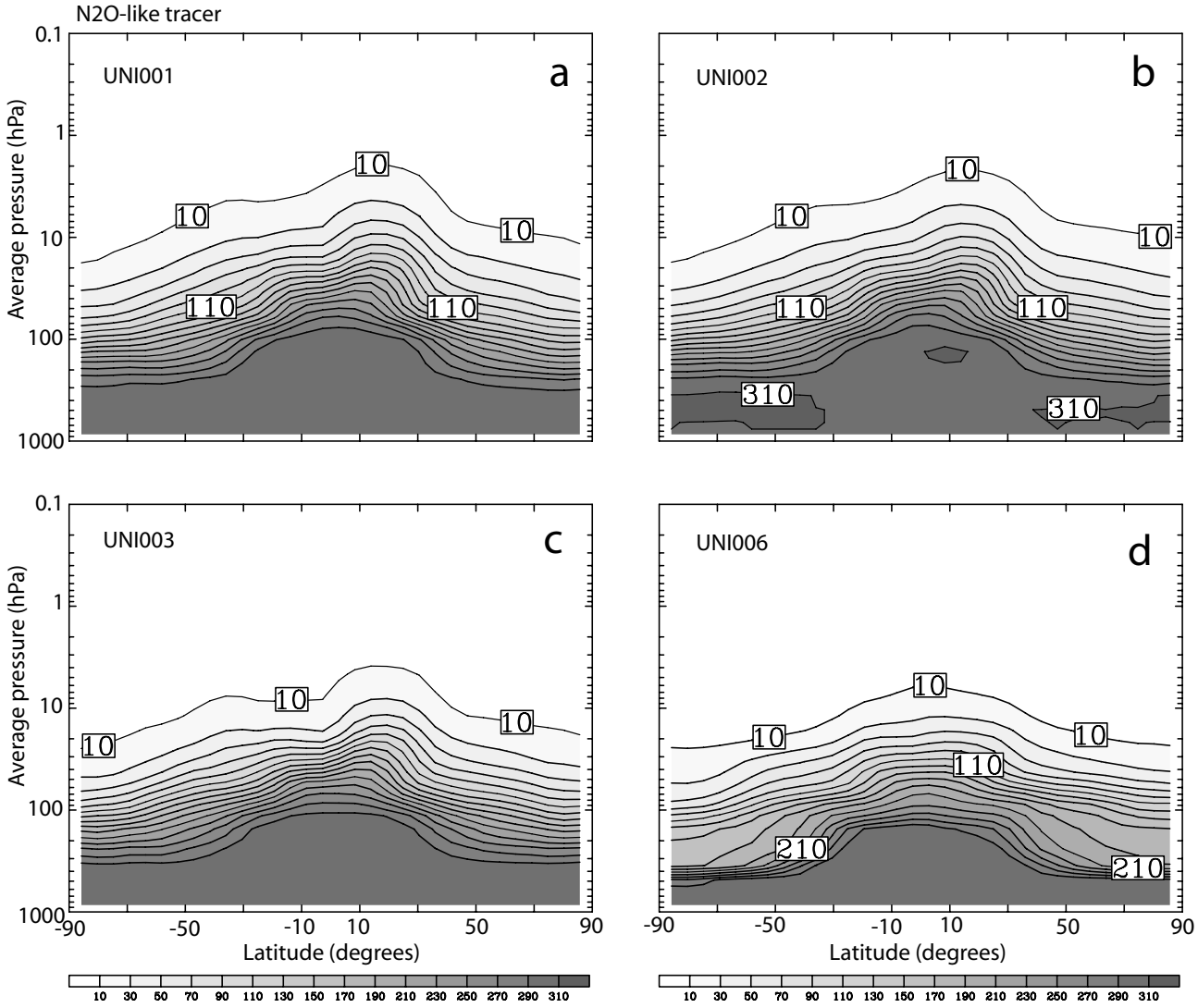

Figure 9. Latitude–height plots of zonal mean annual mean of model 'N_2O-like' tracer for 1992 from the model runs (a) UNI001, (b) UNI002, (c) UNI003, and (d) UNI006. The contour interval is 20 ppbv.

in better agreement with both the balloon and HALOE observations, but the tape-recorder signal in this run decays much too strongly. Overall, the best simulation of both the phase and amplitude, especially when compared to the HALOE data, is given by model run UNI005. Again, this demonstrates that using θ levels in the stratosphere, and diagnosed heating rates for the vertical motion in this regime, produces more realistic vertical transport. This complements the work of Gregory and West (2002) who used a 3D σ-p general-circulation model to show that unrealistic numerical diffusion associated with some advection schemes can cause the tape-recorder signal to propagate too rapidly.

(*c*) *Idealized N_2O-like tracer*

In addition to the completely passive 'age' tracers, the model runs contained a tracer which is similar to a source gas which is long-lived in the LS but photochemically destroyed at higher levels. Figure 9 shows results from this N_2O-like tracer for certain model experiments which showed a large variation in age of air and for two different advection schemes. Clearly, the fact that these tracers have a stratospheric sink and therefore tend to zero in the mid/upper stratosphere means that overall the tracer distributions are much more similar, although differences remain in the LS.

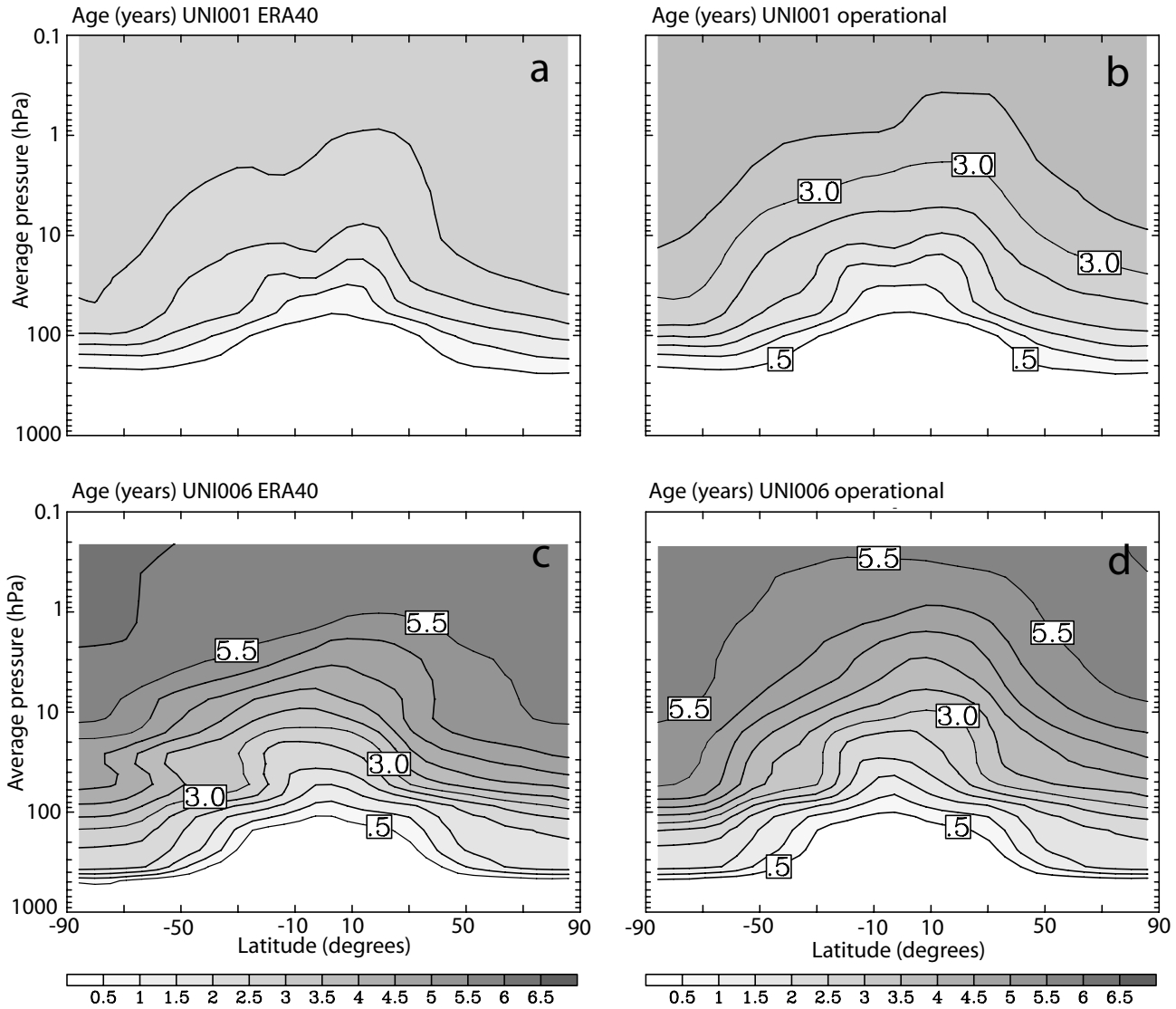

Figure 10. Latitude–height plots of the annual mean zonal mean age of air for 2005 (i.e. after 4 years of repeating 2001 meteorology) for run UNI001 with (a) ERA-40 winds and (b) ECMWF operational winds. (c, d) are as (a, b) but from run UNI006. The contour interval is 0.5 years.

The SLT advection scheme, as used here, creates spuriously large tropospheric mixing ratios due to overshoots in the cubic interpolation, which is undesirable. These overshoots could be easily prevented, but that would make the scheme more diffusive and, importantly, would destroy tracer–tracer correlations.

(*d*) *ERA-40 versus operational winds*

Figure 10 shows the calculated age of air from model run UNI001 for 2001 meteorology using both ERA-40 and operational ECMWF analyses. For 2001, the ERA-40 winds give a different, and slightly greater, stratospheric age compared with the 1992 meteorology shown in Fig. 3. However, there are larger differences between the two sets of analyses. The operational 4D variational analyses produce an age of air which is around 1 year greater than the ERA-40 re-analyses in the US, which were produced using the less-sophisticated 3D-Var system (A. Simmons 2004, personal communication), although the age is still too low. Meijer *et al.* (2004) used a 3D CTM to

show that, for forecast fields, ERA-40 winds also give a lower age of air than operational analyses.

6. Conclusions

This paper has described the development of a new, combined version of the TOMCAT/SLIMCAT 3D CTM. The new CTM has a novel, flexible vertical coordinate which can use both σ-p and σ-θ levels. The CTM has different options for calculating vertical transport in the stratosphere, depending on the coordinate chosen. The CTM also has different options for other processes such as advection scheme, radiation scheme and meteorological forcing.

We have used different configurations of the new CTM to perform tests on stratospheric tracer transport. Using ECMWF ERA-40 re-analyses, the σ-p coordinate model gives a stratospheric age of air which is much too low, and a tropical tape-recorder signal which propagates vertically too rapidly. Changing the coordinates to σ-θ levels, and still using the analyses to calculate the vertical motion, improves the modelled age of air significantly, although it still tends to underestimate the observations. If we use a radiation scheme to calculate the stratospheric diabatic transport in the σ-θ model, we get a greater age of air, and the best overall agreement with the observations of age of air from *in situ* data and estimates of the tape-recorder signal from HALOE. Although the σ-θ model produces more realistic tracer fields, the choice of model coordinate may still depend on the problem being studied. In particular, problems of mass conservation in σ and θ coordinates, and the ease of achieving conservation in p coordinates, can still mean the σ-p coordinate model is useful for some stratospheric studies.

Changing the resolution of the model, while keeping the same forcing winds, can change the modelled age of air. The effect of doubling the resolution was generally small for the relatively non-diffusive Prather (1986) advection scheme. Larger differences were seen with the SLT scheme. These tests indicate the importance of testing a range of model diagnostics rather than just relying on one. Although increasing the horizontal resolution of an off-line model is expected to improve the overall simulation, this decreased the age of air in the tropical US from values which are already too low in some cases.

The modelled zonal mean age of air varies interannually by about 1 year. The current observational database for age of air does not allow us to resolve such a signal. In the future, a larger set of observations should allow us to verify such a signal. In the meantime, these differences should be noted when intercomparing models and when comparing models with data. For a critical test of a CTM with tracer data, it might be important to use analyses from the correct year rather than climatological fields. If the modelled variability is realistic, this will also place limitations on combining sparse datasets from observations made in different years.

For the year 2001, where both sets of analyses are available, the ECMWF operational analyses produce an greater stratospheric age of air than the ERA-40 re-analyses. The ERA-40 re-analyses clearly have a meridional circulation which is too strong. This will cause problems if they are used in a p-coordinate CTM for long-term integrations where vertical motion is taken from the analyses. Our results show, however, that the ERA-40 dataset can still be successfully used in a θ-coordinate model which diagnoses its vertical motion from heating rate. They can be used, for example, as a basis for chemical sensitivity experiments where the analyses provide the model with a good estimate of the meteorological conditions against which one can test the effect of chemical processes. Direct use of ERA-40 winds for transport diagnostics requires some care.

Overall, the various CTM results confirm that the best model formulation for long-term stratospheric simulations with analysed winds is to use θ levels in the stratosphere and heating rates to diagnose the vertical motion. This is the method adopted in the default SLIMCAT CTM which has performed well in simulating details of stratospheric chemistry and this study provides justification for this approach.

ACKNOWLEDGEMENTS

I am very grateful to Pascal Simon (Météo-France) for help with the transport model, especially in the early days in Toulouse. I thank the UK Natural Environment Research Council for an Advanced Research Fellowship which permitted the development of this model. I thank J. Thuburn, K. P. Shine, and B. Briegleb for supplying their radiation schemes and A. Iwi and W. Tian for help with the HALOE tape-recorder data. I am grateful for the use of the OMS balloon data. I thank the two anonymous reviewers for their helpful comments.

APPENDIX

TABLE A.1. DEFINITION OF SYMBOLS

Symbol	Meaning	Value/units
A, B	Parameters to define σ-p levels	
a	Radius of the earth	m
C	Parameter to define σ-θ levels	
c_p	Heat capacity of dry air	1005.46 J kg^{-1}
D_{m}	Mass flux divergence	kg m^{-2}s^{-1}
g	Gravitational acceleration	m s^{-2}
k (subscript)	Model level	
p	Pressure	Pa
p_{s}	Surface pressure	Pa
p_{top}	Pressure at top model interface	Pa
p_θ	Pressure at θ level	Pa
p_0	Reference pressure	100000 Pa
Q	Diabatic heating rate	K s^{-1}
R	Gas constant	287.05 J kg^{-1}
T	Temperature	K
T_{s}	Surface temperature	K
t	Time	s
u	East–west wind	m s^{-1}
v	North–south wind	m s^{-1}
$\mathbf{v}$	Horizontal wind vector	m s^{-1}
w	Vertical velocity	Pa s^{-1}
w_{m}	Vertical mass flux	kg m^{-2}s^{-1}
w_{m0}	Vertical mass flux at top interface	kg s^{-1}
z	Geopotential height	m
η	General dimensionless vertical coordinate	0–1
θ	Potential temperature	K
θ_0	Reference θ	e.g. 350 K
κ	Ratio R/c_p	
λ	Longitude	radians
λ_{w}	Wavelength	m
σ	Terrain-following level	
ϕ	Latitude	radians

REFERENCES

Andrews, A. E., Boering, K. A., Daube, B. C., Wofsy, S. C., Loewenstein, M., Jost, H., Podolske, J. R., Webster, C. R., Herman, R. L., Scott, D. C., Flesch, G. J., Moyer, E. J., Elkins, J. W., Dutton, G. S., Hurst, D. F., Moore, F. L., Ray, E. A., Romashkin, P. A. and Strahan, S. E. 2001 Mean ages of stratospheric air derived from in situ observations of CO_2, CH_4, and N_2O. *J. Geophys. Res.*, **106,** 32295–32314

Boering, K. A., Wofsy, S. C., Daube, B. C., Schneider, H. R., Loewenstein, M., Podolske, J. R. and Conway, T. J. 1996 Stratospheric transport rates and mean age distribution derived from observations of atmospheric CO_2 and N_2O. *Science*, **274,** 1340–1343

Briegleb, B. P. 1992 Delta-Eddington approximation for solar radiation in the NCAR Community Climate Model. *J. Geophys. Res.*, **97,** 7603–7612

Chipperfield, M. P., Cariolle, D., Simon, P., Ramaroson, R. and Lary, D. J. 1993 A three-dimensional modelling study of trace species in the Arctic lower stratosphere during winter 1989–90. *J. Geophys. Res.*, **98,** 7199–7218

Chipperfield, M. P. and Jones, R. L. 1999 Relative influences of atmospheric chemistry and transport on Arctic O_3 trends. *Nature*, **400,** 551–554

Chipperfield, M. P., Santee, M. L., Froidevaux, L., Manney, G. L., Read, W. G., Waters, J. W., Roche, A. E. and Russell, J. M. 1996 Analysis of UARS data in the southern polar vortex in September 1992 using a chemical transport model. *J. Geophys. Res.*, **101,** 18861–18881

Chipperfield, M. P. 1999 Multiannual simulations with a three-dimensional chemical transport model. *J. Geophys. Res.*, **104,** 1781–1805

2003 A three-dimensional model study of long-term mid-high latitude lower stratosphere ozone changes. *Atmos. Chem. Phys.*, **3,** 1–13

Feng, W., Chipperfield, M. P., Davies, S., Sen, B., Toon, G., Blavier, J. F., Webster, C. R., Volk, C. M., Ulanovsky, A., Ravegnani, F., von der Gathen, P., Jost, H., Richard, E. C. and Claude, H. 2005 Three-dimensional model study of the Arctic ozone loss in 2002/2003 and comparison with 1999/2000 and 2003/4. *Atmos. Chem. Phys.*, **5,** 139–152

Fisher, M., O'Neill, A. and Sutton, R. 1993 Rapid descent of mesospheric air into the stratospheric polar vortex. *Geophys. Res. Lett.*, **20,** 1267–1270

Elkins, J. W., Fahey, D. W., Gilligan, J. M., Dutton, G. S., Baring, T. J., Volk, C. M., Dunn, R. E., Myers, R. C., Montzka, S. A., Wamsley, P. R., Hayden, A. H., Butler, J. H., Thompson, T. M., Swanson, T. H., Dlugokencky, E. J., Novelli, P. C., Hurst, D. F., Lobert, J. M., Ciciora, S. J., McLaughlin, R. J., Thompson, T. L., Winkler, R. H., Fraser, P. J., Steele, L. P. and Lucarelli, M. P. 1996 Airborne gas chromatograph for *in situ* measurements of long-lived species in the upper troposphere and lower stratosphere. *Geophys. Res. Lett.*, **23,** 347–350

Eluszkiewicz, J., Helmer, R. S., Mahlman, J. D., Bruhwiler, L. and Takacs, L. L. 2000 Sensitivity of age-of-air calculations to the choice of advection scheme. *J. Atmos. Sci.*, **57,** 3185–3201

Giannakopoulos, C., Chipperfield, M. P., Law, K. S. and Pyle, J. A. 1999 Validation and intercomparison of wet and dry deposition schemes using Pb-210 in a global three-dimensional off-line chemical transport model. *J. Geophys. Res.*, **104,** 23761–23784

Gregory, A. R. and West, V. 2002 The sensitivity of a model's stratospheric tape recorder to the choice of advection scheme. *Q. J. R. Meteorol. Soc.*, **128,** 1827–1846

Hack, J. J., Boville, B. A., Briegleb, B. P., Kiehl, J. T., Rasch, P. J. and Williamson, D. L. 1993 Description of the NCAR Community Climate Model (CCM2), Technical Note NCAR/TN-382+STR, NCAR, Boulder, USA

Hall, T. M., Waugh, A. W., Boering, K. A. and Plumb, R. A. 1999 Evaluation of transport in stratospheric models. *J. Geophys. Res.*, **104,** 18815–18839

Harnisch, J., Borchers, R., Fabian, P. and Maiss, M. 1996 Tropospheric trends for CF_4 and C_2F_6 since 1982 derived from SF_6 dated stratospheric air. *Geophys. Res. Lett.*, **23,** 1099–1102

Holtslag, A. A. M. and Boville, B. 1993 Local versus nonlocal boundary layer diffusion in a global climate model. *J. Climate*, **6,** 1825–1842

Jöckel, P., von Kuhlmann, R., Lawrence, M. G., Steil, B., Bernninkmeijer, C. A. M., Crutzen, P. J., Rasch, P. J. and Eaton, B. 2001 On a fundamental problem in implementing flux-form advection schemes for tracer transport in 3-dimensional general circulation and chemistry transport models. *Q. J. R. Meteorol. Soc.*, **127,** 1035–1052

Kaye, J. A., Douglass, A. R., Rood, R. B., Stolarski, R. S., Newman, P. A., Allen, D. J., Larson, E. M., Coffey, M. T., Mankin, W. G. and Toone, G. C. 1990 Three-dimensional simulation of hydrogen chloride and hydrogen fluoride during the Airborne Arctic Stratospheric Expedition. *Geophys. Res. Lett.*, **17,** 529–532

Law, K. S., Plantevin, P.-H., Shallcross, D. E., Rogers, H. L., Pyle, J. A., Grouhel, C., Thouret, V. and Marenco, A. 1998 Evaluation of modeled O_3 using Measurements of Ozone by Airbus In-Service Aircraft (MOZAIC) data. *J. Geophys. Res.*, **103,** 25721–25737

Lefèvre, F., Brasseur, G. P., Folkins, I., Smith, A. K. and Simon, P. 1994 Chemistry of the 1991-1992 stratospheric winter: Three-dimensional model simulations. *J. Geophys. Res.*, **99,** 8183–8195

Louis, J.-F. 1979 A parametric model of vertical eddy fluxes in the atmosphere. *Boundary-Layer Meteorol.*, **17,** 187–202

Mahowald, N. M., Plumb, R. A., Rasch, P. J., del Corral, J., Sassi, F. and Heres, W. 2002 Stratospheric transport in a three-dimensional isentropic coordinate model. *J. Geophys. Res.*, **107,** doi: 10.1029/2001JD001313

Mann, G. W., Davies, S., Carslaw, K. S., Chipperfield, M. P. and Kettleborough, J. 2002 Polar vortex concentricity as a controlling factor in Arctic denitrification. *J. Geophys. Res.*, **107,** 4663, doi: 10.1029/2002JD002102

Meijer, E. W., Bregman, B., Segers, A. and van Velthoven, P. F. J. 2004 The influence of data assimilation on the age of air calculated with a global chemistry-transport model using ECMWF wind fields. *Geophys. Res. Lett.*, **31,** L23114, doi: 10.1029/2004GL021158

Norton, W. A. and Iwi, A. 1999 'Validation of chemical transport models by tape recorder and age diagnostics'. Pp. 562–565 in Proceedings of Fifth European Symposium on Stratospheric Ozone, St Jean de Luz, September 1999. (EC Air Pollution Research Report No. 73)

Prather, M. J. 1986 Numerical advection by conservation of second-order moments. *J. Geophys. Res.*, **91,** 6671–6681

Ray, E. A., Moore, F. L., Elkins, J. W., Dutton, G. S., Fahey, D. W., Vömel, H., Oltmans, S. J. and Rosenlof, K. H. 1999 Transport into the Northern Hemisphere lowermost stratosphere revealed by *in situ* tracer measurements. *J. Geophys. Res.*, **104,** 26565–26580

Rotman, D. A., Atherton, C. S., Bergmann, D. J., Cameron-Smith, P. J., Chuang, C. C., Connell, P. S., Dignon, J. E., Franz, A., Grant, K. E., Kinnison, D. E., Molenkamp, C. R., Proctor, D. D. and Tannahill, J. R. 2004 IMPACT, the LLNL 3D global atmospheric chemical transport model for the combined troposphere and stratosphere: Model description and analysis of ozone and other trace gases. *J. Geophys. Res.*, **109,** doi: 10.1029/2002JD003155

Rood, R. B., Allen, D. J., Baker, W. E., Lamich, D. J. and Kaye, J. A. 1989 The use of assimilated stratospheric data in constituent transport calculations. *J. Atmos. Sci.*, **46,** 687–701

Russell, G. L. and Lerner, J. A. 1981 A new finite differencing scheme for the tracer transport equation. *J. Appl. Meteorol.*, **20,** 1483–1498

Schoeberl, M. R., Douglass, A. R., Zhu, Z. and Pawson, S. 2003 A comparison of the lower-stratospheric age spectra derived from a general circulation model and two data assimilation systems. *J. Geophys. Res.*, **108,** doi: 10.1029/2002JD002652

Segers, A., van Velthoven, P., Bregman, B. and Krol, M. 2002 'On the computation of mass fluxes for Eulerian transport models from spectral meteorological fields'. Pp. 767–776 in Proceedings (Part 2) of the 2002 International Conference on Computational Science, Amsterdam. *Lecture Notes in Computer Science*, Springer-Verlag

Shine, K. P. 1987 The middle atmosphere in the absence of dynamical heat fluxes. *Q. J. R. Meteorol. Soc.*, **113,** 603–633

1989 Zonal momentum in the middle atmosphere. *Q. J. R. Meteorol. Soc.* **115,** 265–292

Shine, K. P. and Rickaby, J. A. 1989 'Solar radiative heating due to absorption by ozone'. Pp. 597–600 in Proceedings of Quadrennial Ozone Symposium, Göttingen. A. Deepak, Hampton, Va., USA

Staniforth, A. and Coté, J. 1991 Semi-Lagrangian integration schemes for atmospheric models—A review. *Mon. Weather Rev.*, **119,** 2206–2223

Stockwell, D. Z. and Chipperfield, M. P. 1999 A tropospheric chemical transport model: Development and validation of the model transport schemes. *Q. J. R. Meteorol. Soc.*, **125,** 1747–1783

Stockwell, D. Z., Giannakopoulos, C., Plantevin, P. H., Carver, G. D., Chipperfield, M. P., Law, K. S., Pyle, J. A., Shallcross, D. E. and Wang, K. Y. 1999 Modelling NOx from lightning and its impact on global chemical fields. *Atmos. Environ.*, **33**(27)**,** 4477–4493

Swinbank, R. and O'Neill, A. 1994 A stratosphere–troposphere data assimilation system. *Mon. Weather Rev.*, **122,** 686–702

Thuburn, J. T. 1993 Baroclinic wave life-cycles, climate simulations and cross-isentropic mass flow in a hybrid isentropic coordinate GCM. *Q. J. R. Meteorol. Soc.*, **119,** 489–508

Tiedtke, M. 1989 A comprehensive mass flux scheme for cumulus parameterization in large-scale models. *Mon. Weather Rev.*, **117,** 1779–1800

Uppala, S. M., Kållberg, P. W., Andrae, U., da Costa Bechtold, V., Fiorino, M., Hernandez, A., Li, X., Onogi, K., Saarinen, S. and Sokka, N. 2004 'ERA-40: ECMWF 45-year reanalysis of the global atmosphere and surface conditions 1957–2002'. Newsletter No. 101, ECMWF, Reading, UK

Waugh, D. W. and Hall, T. M. 2002 Age of stratospheric air: Theory, observations and models. *Rev. Geophys.*, **40,** doi: 10.1029/2000RG00101

Wang, K.-Y., Pyle, J. A., Sanderson, M. G. and Bridgeman, C. 1999 Implementation of a convective atmospheric boundary layer scheme in a tropospheric chemistry transport model. *J. Geophys. Res.*, **104,** 23729–23745

Weaver, C. J., Douglass, A. R. and Rood, R. B. 1993 Thermodynamic balance of three-dimensional stratospheric winds derived from a data assimilation procedure. *J. Atmos. Sci.*, **50,** 2987–2993

2000 Lamination frequencies as a diagnostic for horizontal mixing in a 3D transport model. *J. Atmos. Sci.*, **57,** 247–261

Williamson, D. L. and Rasch, P. J. 1989 Two-dimensional semi-Lagrangian transport with shape-preserving interpolation. *Mon. Weather Rev.*, **117,** 102–129

Zapotocny, T. H., Johnson, D. R., Reames, F. M., Pierce, R. B. and Wolf, B. J. 1991 Numerical investigations with a hybrid isentropic-sigma model. Part II: The inclusion of moist processes. *J. Atmos. Sci.*, **48,** 2025–2043